Model-based investigation of transmural gradients in activation rate during ventricular fibrillation

Patrick M. Boyle^a, Kumar Nanthakumar^b, Edward J. Vigmond^a

^aUniversity of Calgary, Calgary, Canada ^bUniversity Health Network, Toronto, Canada

Correspondence: PM Boyle, Department of Electrical & Computer Engineering, University of Calgary, 2500 University Dr. NW, Calgary AB T2N 1N4, Canada. E-mail: pmjboyle@gmail.com, phone +1 403 220 8798, fax +1 403 282 6855

Abstract. Experimental models of ventricular fibrillation (VF) suggest that a transmural gradient in the rate of activation develops, usually with faster activation near terminal sites of the Purkinje system (PS), but the underlying mechanism of this phenomenon is not well understood. A computer model of the rabbit ventricles with and without the PS was used to investigate the major cell- and tissue-level factors that influence the development of this sort of heterogenity. Variation of parameters associated with modelling the effects of global ischemia was explored to produce test cases with different gradients of action potential duration (APD) shortening between the endocardial and epicardial surfaces. Simulation results suggest that a large difference in APD brought about by a steep gradient in ischemic activation of ATP-sensitive potassium channels, is necessary to overcome electrotonic effects in tissue andachieve significantly different activation rates across the ventricular wall during VF. Inclusion of the PS changed activation patterns but did not affect the likelihood of gradient formation. Understanding how rate gradients form in adjacent tissue regions will help explain complex phenomena associated with cardiac arrhythmia, such as synchronized endocardial activation during episodes of long-duration VF.

Keywords: ventricular fibrillation, transmural activation rate gradient, Purkinje system, global ischemia, action potential duration, ATP-sensitive potassium channels, computer models.

1. Introduction

Ventricular fibrillation (VF) is a major cause of death but its underlying mechanisms are not completely understood. Experiments in the porcine model have described regional differences in activation rate in fibrillating ventricles, with higher dominant frequency (DF) on the epicardium compared to the endocardium [Nanthakumar et al., 2002]. Furthermore, periods of highly synchronized endocardial activation are known to occur late in long-duration VF while the ECG maintains a chaotic pattern [Robichaux et al., 2010]; understanding how activity in adjoining cardiac regions becomes uncoordinated or completely isolated could help explain this phenomenon.

During VF, effective contraction is impaired and perfusion of the heart via the coronary arteries ceases, which leads to the gradual development of global ischemia. This condition is associated with acute remodeling at the cell membrane level, which results in shortened action potential duration (APD) throughout the ventricles; regional heterogeneity in the extent of ischemic effects is thought to be a crucial factor in maintaining the reentrant circuits that underlie VF [Furukawa et al., 1991].

Despite the importance of understanding how VF behaves, the exact mechanism of spatial heterogeneity of activation rates remains an unanswered question. Variation in single-cell properties does not necessarily translate into regional differences, since electrotonic interaction in tissue can have a smoothing effect. In this study, we used computer modeling to test the hypothesis that a large difference in intrinsic APD is necessary to achieve a significant transmural gradient in activation rate during VF. Simulations were performed with and without a model of the Purkinje system (PS) to assess whether the presence of conductive tissue near the epicardium promotes transmural heterogeneity.

2. Material and Methods

2.1. Computer model of ventricles and Purkinje system

Our basis for simulating the biophysics of cardiac electrophysiology is described in detail elsewhere [Boyle et al., 2010]. Briefly, experiments were carried out on a tetrahedral representation of the ventricles based on rabbit geometry [Vetter & McCulloch, 1998] (862,515 nodes including tissue, surrounding medium, and cavities; mean edge length of 250 μ m). Tissue was modeled with anisotropic conductivity values from [Clerc, 1976]; fiber orientations were extracted from histological slices. Baseline ionic kinetics in ventricular cells were governed by the equations of [Mahajan, Shiferaw, et al., 2008] with an adenosine triphosphate-sensitive potassium current ($I_{K(ATP)}$) [Ferrero et al., 1996].

The PS model was an adapted version of the anatomically-based branching network of 1D cubic Hermite elements from [Vigmond & Clements, 2007], modified to terminate subepicardially in the case of free wall Purkinje-myocardial junctions (PMJs) or deep in the myocardium in the case of septal PMJs. PS endpoints were coupled to 60-80 surrounding myocardial nodes and the two systems were linked by anterograde and retrograde current, with junctional parameters tuned to reproduce propagation delays on the same order as those observed experimentally. Purkinje fiber membrane properties were described by the [Aslanidi, Sleiman, et al., 2010] model.

During the application of electric shocks, the distribution of potential and current in tissue was governed by the bidomain formulation; otherwise, a monodomain simplification was used to simplify computation. This has been shown to produce negligible differences in results [Potse et al., 2006].

2.2. Global ischemia parameters

To model the progressive effects of no-flow ischemia in ventricular cells, we modified a regional model of ischemia phase 1A [Tice et al., 2007]. Border zones were removed, since they do not exist in global ischemia. Since glycogen reserves in Purkinje fibers limit acute effects of oxygen deprivation, no ischemic effects were incorporated in the PS. In the Tice model of ischemia, extracellular potassium concentration ($[K^+]_e$) and the fraction of open $I_{K(ATP)}$ channels (f_{ATP}) increased over time while maximal sodium and calcium channel conductances (g_{Na} and $g_{Cal.}$) decreased. Based on existing characterizations of ischemia, sub-epicardial $[K^+]_e$ and sub-endocardial f_{ATP} were set to 60% elevation with respect to maximum levels, creating oppositely oriented linear gradients.

We performed a sensitivity analysis to determine the optimal modification of parameters in the ischemia model for producing large differences between maximum activation rate for single epicardial and endocardial cells without reducing epicardial APD to non-physiological levels. Dynamic restitution experiments to assess minimum APD were conducted for both cell types for each combination of ischemic time (t_{isch}), maximal f_{ATP} , and gradient steepness for f_{ATP} and $[K^+]_e$.

2.3. Recovery and analysis of extracellular potentials

Extracellular potentials (ϕ_e) at several points near the epicardial surface (see Fig. 1) were recovered by integrating the effects of transmembrane current in the volume of the heart. Recordings from the right and left basal ventricles and the apex were differenced to construct pseudo-ECG signals; paired endocardial and epicardial sites were positioned in emulation of basket catheters and so-called electrode socks, which are commonly used in experimental settings.

To assess activation rates during VF, DF analysis was performed on unipolar and bipolar recordings from endocardial and epicardial sites with a standard technique [Zaitsev, 2000]. Signals sampled at 1 kHz were low-pass filtered using an elliptic FIR with 60 Hz cutoff then decimated to 125 samples per second and divided into 1-second epochs. For each group of two adjacent epochs, a 250-point Hamming-windowed FFT was applied and the highest component between 3 and 14 Hz was called the DF. These values were compared between adjacent endocardial and epicardial points to establish whether a transmural gradient was present.

To confirm epicardial and endocardial rate gradients, DF analysis was also carried out on sets of bipolar recordings, which were generated from adjacent pairs of leads. Furthermore, membrane voltage (V_m) traces from myocardial nodes near basket and sock recording sites were directly inspected to count activations, which were defined by threshold crossing (-20 mV) with a 40 ms blanking interval.

2.4. Simulation protocol

Reentry was induced using an S1-S2 protocol, as described elsewhere [Deo, 2009]. S1 was the last in a sequence of several sinus beats (periodic His bundle stimulation) and S2 was a large electric field along the septum some time later. For each set of parameters tested, the coupling interval between the

two stimuli was iteratively adjusted to find the shock that induced lasting arrhythmia. Monodomain simulations took approximately 1.5 hours per simulated second on a cluster of 12 CPUs clocked at 1.6 GHz. On the same hardware, simulations incorporating the bidomain formulation took approximately 35x longer, but this was only used during shocks (3 ms) and a short interval afterwards (7 ms).

3. Results

3.1. Sensitivity analysis

A recent optical mapping study showed that realistic minimum epicardial APD during VF for rabbits was in the range of 80 ms [Harada, 2011]. We found that this value was highly sensitive to changes in maximal f_{ATP} ; as such, we limited our search in the other two parameters to cases where $f_{ATP,max} = 0.4$, which corresponds to a minimum epicardial APD range between 70 and 95 ms.

Within this subset of parameter space, the only variations that resulted in significant transmural APD gradients for single cells were increases in fATP gradient steepness and drastic increases in t_{isch}, associated with across-the-board increases in ischemic modifications. Figure 1 compares dynamic restitution curves for the baseline parameter set ($t_{isch} = 4$ minutes, default gradient steepness of 0.6) and a set with f_{ATP} gradient steepness increased to 0.0, which increased the gradient between minimal endocardial and epicardial APD by 16 ms. These two parameter sets were integrated in the whole heart model and VF was induced to the gradient would overcome electrotonic coupling effects to persist as differences in activation rate.

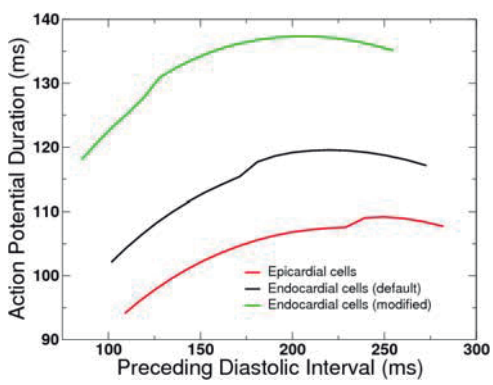


Fig. 1 Dynamic restitution properties with and without modifications to steepen endocardial-to-epicardial APD gradient.

3.2. Ventricular fibrillation

For the both sets of ischemia parameters (baseline and modified, as described in §3.1) reentry was induced for a coupling interval of 140 ms with the PS and 142 ms without. In all cases, wavebreak occurred in short order and distribution of excitation became disorganized, as in VF. Figure 2 shows simultaneous epicardial and endocardial snapshots during a well-established episode of VF. While qualitative assessment of activation rate is difficult, there are clearly more wavefronts on the heart's outer surface and their wavelengths appear to be shorter than those on the inner surface.

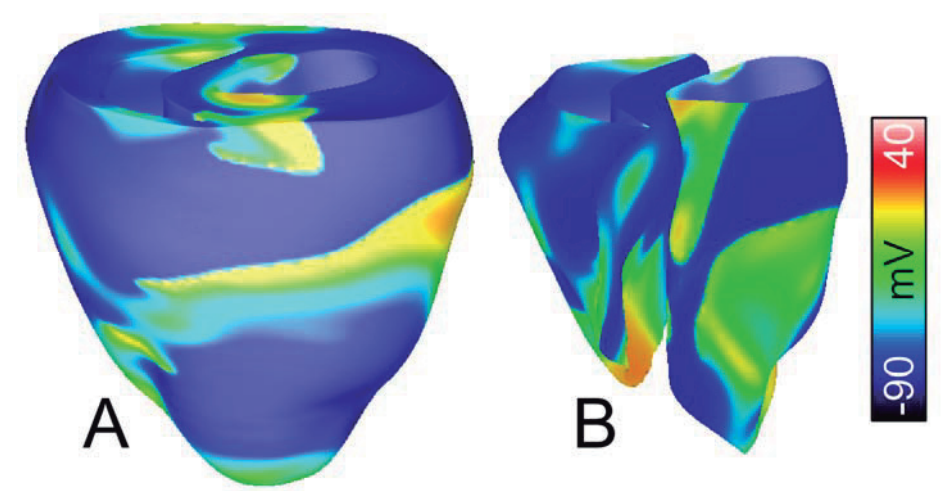


Fig. 2: V_m maps of VF on the epicardium (A) and endocardium (B) during an episode of VF with parameters modified to steepen endocardial-to-epicardial APD gradient. The outer surface of the heart, where $I_{K(ATP)}$ effects are highest, has a larger number of shorter wavefronts.

Notable effects of the PS during VF are shown in Fig. 3. Breakthroughs from subepicardial PMJs occurred frequently and led to new wavefronts, but this did not appear to have a significant affect in terms of acceleration of the epicardial rate. In many cases, the longer intrinsic APD of Purkinje fibres resulted in regions of prolonged myocardial refractoriness surrounding junctions; these affected VF wavefronts in many ways, extinguishing some and providing functional obstacles for new scroll waves in others.

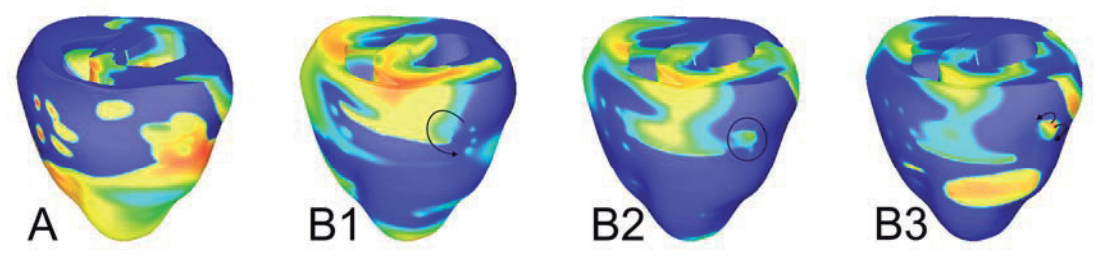


Fig. 3: Effects of the sub-epicardially penetrating PS during VF. In addition to regular breakthroughs (A), refractoriness around PMJs causes wavebreak. In B, part of an existing rotor is "pinched off" (B1) and slowed down (B2), resulting in reentry around the functional obstacle (B3). Colour scale as in Fig. 2.

3.3. Dominant frequency analysis

For the baseline set of parameters, which had an intrinsic APD difference of 8 ms, no significant gradient between epicardial and endocardial activation rates was detected during VF. In contrast, for VF with modified parameters, where APDs were 24 ms shorter on the epicardium than on the endocardium, all DF analysis methods calculated a significant transmural gradient. As shown in Fig. 4, the mean activation rate was approximately 2 Hz higher on the epicardium than on the endocardium.

Although the different DF analysis methods produced similar average values, FFT-based techniques were considerably more variable when compared to directly counting activations. No statistical analysis was performed to confirm the difference in means between populations, but the similar levels found by the $V_{\rm m}$ -based method suggested the difference method is accurate.

Inclusion of the PS did not appear to significantly affect the formation of transmural gradients in activation rate.

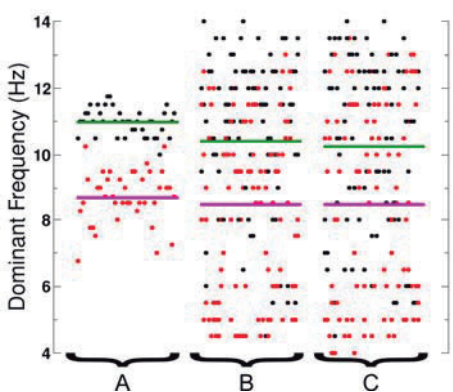


Fig. 4: DF values obtained by counting V_m activations (A) or performing windowed FFTs on unipolar (B) and bipolar (C) recordings. Endocardial (black) and epicardial (red) points from patched pairs are vertically adjacent. Means for all epicardial (green) and endocardial (magenta) values are shown.

4. Discussion & conclusions

The simulations performed in this study demonstrate that a large intrinsic difference in APD must exist between epicardial and endocardial cells in order for a significant transmural activation rate gradient to be present during VF. With baseline ischemia parameters, derived from an established model of ischemia and modified to limit minimum epicardial APD to a reasonable value, a nominal APD difference of 8 ms was handily suppressed during VF, presumably due to electrotonic effects. In contrast, when the intrinsic APD difference was exacerbated by steepening the gradient of f_{ATP} expression, epicardial activation during VF was approximately 2 Hz faster than endocardial activation. Notably, the average DFs calculated correspond quite well with the theoretical maximum epicardial and endocardial values of 10.63 and 8.47 Hz based on single-cell restitution experiments.

The FFT-based approach to DF analysis produced highly variable results for both unipolar and bipolar recordings. Although mean values were tentatively validated by comparison with DFs calculated by directly counting activations, the distribution of points in Fig. 4B and C is troubling. A detailed analysis of application of this method to simulation results is warranted and comparison to the results of applying the same tool to data from experiments would also be informative.

Although these results demonstrate the importance of an intrinsic difference in APD to the formation of transmural gradients in activation rates, they do not purport to be a comprehensive investigation of the phenomenon. Indeed, analysis of VF simulations was restricted to a two-sample subset of the parameter space representing relatively extreme cases. Future studies should attempt to identify threshold levels of single-cell difference for overcoming the smoothing effects of electrotonic interaction to create organ-level heterogeneity. Furthermore, some physiological details, including subepicardial PS penetration and enhanced epicardial $I_{K(ATP)}$ expression, may have different effects when simulated in the context of pig electrophysiology and geometry. In particular, the increase in size might promote transmural rate gradients for lower intrinsic APD differences.

Acknowledgments

This research was supported by the Natural Sciences and Engineering Research Council of Canada (NSERC) and the Mathematics of Information Technology and Complex Systems (MITACS) Network of Centers of Excellence.

References

Aslanidi OV, Sleiman RN, Boyett MR, et al. Ionic mechanisms for electrical heterogeneity between rabbit Purkinje fiber and ventricular cells. *The Biophysical Journal*, 98: 2420-2431, 2010.

Boyle PM, Deo M, Plank G, Vigmond EJ. Purkinje-mediated effects in the response of quiescent ventricles to defibrillation shocks. *Annals of Biomedical Engineering*, 38: 456-468, 2010.

Clerc L. Directional differences of impulse spread in trabecular muscle from mammalian heart. *The Journal of Physiology*, 255(2): 335-346, 1976.

Deo M, Boyle P, Plank G, Vigmond EJ. Arrhythmogenic mechanisms of the Purkinje system during electric shocks: a modeling study. *Heart Rhythm*, 6:1782-1789, 2009.

Ferrero JM, Saiz J, Ferrero JM, Thakor NV. Simulation of action potentials from metabolically impaired cardiac myocytes. Role of ATP-sensitive K+ current. *Circulation Research*, 79: 208-21, 1996.

Furukawa T, Kimura S, Furukawa N et al. Role of cardiac ATP-regulated potassium channels in differential responses of endocardial and epicardial cells to ischemia. *Circulation Research*, 68: 1693-702, 1991.

Harada M, Tsuji Y, Ishiguro YS et al. Rate-dependent shortening of action potential duration increases ventricular vulnerability in failing rabbit heart. *American Journal Physiology: Heart and Circulatory Physiology*, 300(2): H565-73, 2011.

Mahajan A, Shiferaw Y, Sato D, et al. A rabbit ventricular action potential model replicating cardiac dynamics at rapid heart rates. *The Biophysical Journal*, 94: 392-410, 2008.

Nanthakumar K, Huang J, Rogers J, et al. Regional differences in ventricular fibrillation in the open-chest porcine left ventricle. *Circulation Research*, 91: 733-740, 2002.

Potse M, Dub B, Richer J, Vinet A, et al. A comparison of monodomain and bidomain reaction-diffusion models for action potential propagation in the human heart. *IEEE Transactions on Biomedical Engineering*, 53: 2425-2435, 2006.

Robichaux RP, Dosdall, DP, Osorio, et al. Periods of highly synchronous, non-reentrant endocardial activation cycles occur during long-duration ventricular fibrillation. *Journal of Cardiovascular Electrophysiology*, 21(11): 1266-73, 2010.

Tice BM, Rodriguez B, Eason J, and Trayanova N. Mechanistic investigation into the arrhythmogenic role of transmural heterogeneities in regional ischaemia phase 1A. *Europace*, 9(S6): vi46-58, 2007.

Vetter F and McCulloch A. Three-dimensional analysis of regional cardiac function: a model of rabbit ventricular anatomy. *Progress in Biophysics and Molecular Biology*, 69: 157-183, 1998.

Vigmond EJ and Clements C. Construction of a computer model to investigate sawtooth effects in the Purkinje system. *IEEE Transactions on Biomedical Engineering*, 54(3): 389-99, 2007.

Zaitsev AV, Berenfeld O, Mironov SF, et al. Distribution of excitation frequencies on the epicardial and endocardial surfaces of fibrillating ventricular wall of the sheep heart. *Circulation Research*, 86: 408-417, 2000.